HEAT UP AND POTENTIAL FAILURE OF BWR UPPER INTERNALS DURING A SEVERE ACCIDENT

K. R. Robb*

Oak Ridge National Laboratory
P.O. Box 2008, Oak Ridge, TN 37830, USA
robbkr@ornl.gov

ABSTRACT

In boiling water reactors, the steam dome, steam separators, and dryers above the core are comprised of approximately 100 tons of stainless steel. During a severe accident in which the coolant boils away and exothermic oxidation of zirconium occurs, gases (steam and hydrogen) are superheated in the core region and pass through the upper internals. Historically, the upper internals have been modeled using severe accident codes with relatively simple approximations. The upper internals are typically modeled in MELCOR as two lumped volumes with simplified heat transfer characteristics, with no structural integrity considerations, and with limited ability to oxidize, melt, and relocate.

The potential for and the subsequent impact of the upper internals to heat up, oxidize, fail, and relocate during a severe accident was investigated. A higher fidelity representation of the shroud dome, steam separators, and steam driers was developed in MELCOR v1.8.6 by extending the core region upwards. This modeling effort entailed adding 45 additional core cells and control volumes, 98 flow paths, and numerous control functions. The model accounts for the mechanical loading and structural integrity, oxidation, melting, flow area blockage, and relocation of the various components. The results indicate that the upper internals can reach high temperatures during a severe accident; they are predicted to reach a high enough temperature such that they lose their structural integrity and relocate. The additional 100 tons of stainless steel debris influences the subsequent in-vessel and ex-vessel accident progression.

KEYWORDS
upper internals, BWR, severe accident, MELCOR

1. INTRODUCTION AND BACKGROUND

Above the core of a boiling water reactor (BWR) are the upper internals (UIs), which consist of the shroud dome, steam separators and steam dryers. They condition the steam before entering the main steam lines. Steam separators are mounted onto the shroud dome, which is approximately 50 mm (2 in.) thick. The steam separators are formed by standpipes, each with a separator section. A device causes the flow to swirl, forcing the droplets in the steam to move towards the walls and be removed. The dryers force the steam through a convoluted flow path, further removing droplets from the steam. These features

are generally common to all BWRs. This paper focuses on the BWR/4 series, which is the BWR type most commonly deployed in the US and is the reactor type of Fukushima Daiichi Units 2 and 3.

During a severe accident, core cooling is not maintained, and the core eventually heats up and melts. During accidents in which the coolant boils away, the steam oxidizes the hot core. The oxidation of zirconium by steam is highly exothermic and contributes to the superheating of the steam and hydrogen. The superheated gases then pass through the UIs on their way out of the reactor pressure vessel (RPV) either through the safety relief valves (SRVs), through the steam lines for steam-driven pumps, or through a break in the piping. In addition to the flow of superheated gases, thermal radiation from a melting core can contribute to heating the shroud dome and steam separators standpipes. It is conceivable for the UI to reach high enough temperatures such that they may begin to lose structural integrity, slump, and possibly even begin melting.

Historically, the UIs have been modeled relatively simply in severe accident codes. For example, in the State-of-the-Art Reactor Consequence Analyses (SOARCA) [1], the UIs were modeled with two 1-D heat structures, three control volumes, and approximately five flow paths. Section 4.2.3 of the report notes: "*A limitation of this modeling approach is that the mechanical response of these structures, material melting or collapse and the potential for incorporation of steel into core debris, is not modeled. Changes in the flow area through this region of the RPV that might be caused by changes in structure geometry are also not modeled*" [1].

Only one past paper could be identified that has specifically investigated the heat up of the UIs during a severe accident [2]. In the work, a standalone model was developed based on finite element methods to evaluate the heat up of the shroud head and the inlets to the steam separators. The model accounted for various modes of convection and thermal radiation heat transfer. The model used boundary conditions, gas flow rates, composition, and temperatures that were calculated from MARCON, a severe accident modeling tool of the time. For the scenario investigated, a long-term station blackout (LTSBO), the results suggested the shroud dome could reach temperatures above 1427°C (2600°F), well above the material's working temperature.

This paper explores the potential for the superheated gases and thermal radiation during a severe accident to heat the UIs to temperatures that may compromise their structural integrity.

2. ANALYSIS SETUP

2.1. Overview of Tools

MELCOR is a system level code that models the progression of severe accidents in light water nuclear power plants [3]. It is developed and maintained by Sandia National Laboratories (SNL) for the US Nuclear Regulatory Commission. The code encompasses various phenomena that can occur during a severe accident, including the thermal-hydraulic response, the heat up, degradation and relocation of the core, transport of radionuclides, and hydrogen generation and combustion. Among its uses, MELCOR is primarily used to estimate the source term from severe accidents. In this study, MELCOR version 1.8.6(.4073) [3], as compiled by SNL, is used on a computer with the Windows operating system and Intel-based hardware.

2.2. Baseline Plant Model Description

The MELCOR plant model used is for Peach Bottom (Unit 2 or 3), a BWR series 4 (BWR/4) with a Mark I containment. The model includes all major components including the reactor, containment, reactor building, the various cooling systems (pumps, sprays, piping, tanks), as well as system and scenario

control logic. The model recently was updated from MELCOR 1.8.5 for use in MELCOR 1.8.6. This update, the model's lineage, and additional model updates have been previously described [4]. Since the update described in Ref. [4], the lower head region was renodalized.

In the base model, before modification, the UIs were modeled as follows. The shroud dome, steam separators, and dryers were modeled with two heat structures. The shroud dome and steam separators were grouped together and modeled with a single heat structure. The heat structure was modeled as a 18.6 mm thick vertical plate weighing approximately 69,700 kg, with a surface area of 472 m^2. The plate was in contact with the flow out of the core, and another 472 m^2 of its surface area was in contact with the downcomer annulus region. The steam dryers were modeled with a single heat structure. The heat structure was modeled as a 1.83 mm thick vertical plate, weighing approximately 42,700 kg with a surface area of 2945 m^2. The plate was in contact with the flow out of the separators, and another 2,945 m^2 of surface area was in contact with the steam dome region. The two heat structures were each located within their own control volumes. Using the MELCOR degassing model option, the separators could melt if the temperature approached 1,700 K. If they were to melt, the material would enter the outer ring of the core region. To model the UIs for the current work, many additions and updates were required as described in Section 2.4.

2.3. Accident Scenario Description

The short term station blackout (STSBO) severe accident scenario was chosen for investigation. During the STSBO scenario, the reactor is assumed to successfully shutdown (reference time 0 h). All AC power, including off-site and on-site power (diesel generators), is assumed to be lost at 0 h. The timing of the loss of DC power (batteries) is assumed to occur at 0 h. Without DC power, the reactor core isolation cooling (RCIC) system and the high pressure coolant injection (HPCI) system cannot be used to inject cooling water into the primary system. In the scenario, water injection into the primary system is not restored. It was assumed that operators did not take action (or that they were unsuccessful) to depressurize the RPV or its containment. The simulations were specified to end 14 hours after reactor shutdown.

The station blackout scenario was chosen due to its high contribution to the overall core damage frequency for BWRs [1, 5]. Furthermore, it is similar to the events at Fukushima Daiichi Units 1–3. In addition, the previous study, which focused specifically on the heat up of the UIs, was based on a station blackout [2], which allows for comparison of the results. The MELCOR model additions to represent the UIs increased the computational time required for simulations by approximately 3.3×. Therefore, due to the shorter duration between phases of the accident, an STSBO was chosen for this scoping study.

2.4. Modeling the BWR Upper Internals in MELCOR

2.4.1. Assumed geometry

Table I summarizes the geometry assumed for the UIs based on information from Refs. [6, 7]. The dimensions are intended to be representative of the geometry of the UIs of a BWR/4 series reactor; however, the actual geometry may vary from that assumed. For the purposes of this scoping study, the assumed geometry is deemed sufficient. Table II summarizes the modeled UI mass. The default density for stainless steel in MELCOR is 7930 kg/m^3.

Table I. Summary of assumed dimensions for upper internals

Parameter	Dimension SI	US Customary
Thickness of shroud head	0.0508 m	2.0 in
Free volume under shroud dome	27.29 m^3	11,564 ft^3
Upper shroud OD	5.588 m	220.0 in
Number of standpipes	211	211
Standpipe ID	0.154 m	6.07 in
Standpipe OD	0.168 m	6.63 in
Separator section OD	0.324 m	12.75 in
Length of standpipe lower section	1.9 m	74.80 in
Length of standpipe separator section	1.85 m	72.84 in
Length of standpipe top section	0.5 m	19.69 in
Free space height above separator	0.75 m	29.53 in
Height of dryers	2.2 m	86.61 in
Thickness of steam dryer support	0.0381 m	1.50 in
Steam dryer hydraulic diameter	0.0127 m	0.50 in
Steam dryer surface area	2,945 m^2	31,700 ft^2

*ID: inner diameter; OD: outer diameter

Table II. Summary of assumed upper internals mass

Component	Mass (kg)	Mass (lb)
Dryers	40,823	90,000
Separators	56,565	124,783
Shroud dome	6,836	15,075
Total	**104,224**	**229,858**

2.4.2. Discretization and modeling representation

Modeling the UIs required approximately 4,500 new lines of code input and the modification of approximately 300 existing lines. The following is a brief description of the methodology used to model the UIs in MELCOR. The purpose of this section is to identify issues encountered when working to model the UIs in MELCOR and provide a starting point for MELCOR users to develop their own models. For non-MELCOR users, this section provides an overview of the compromises made when modeling the UIs and the fidelity of the model.

The shroud dome was represented as a PLATE type support structure (SS). This structure supports the weight of itself and the steam separators.

Different modeling methodologies were identified to represent the steam separators. However, each methodology has unique limitations and approximations. The standpipes could either be modeled as SS or as canister (CN) core components. If the standpipes were modeled as CN components, the space outside the standpipes would be modeled as bypass regions. If the standpipes were modeled as SS, the space outside the standpipes would need to be modeled using control volumes external to the COR package.

Table III summarizes the identified benefits and drawbacks of modeling the standpipes as either SS or CN components.

Table III. Comparison of methodologies for modeling the steam separator standpipes

Category	Supporting structure	Canister
Material	Structure and canister materials can be appropriately specified	All canisters in core must be same material
Structural loading	Models structural loading and failure mechanisms	Does not model structural loading failure mechanisms
Convection heat transfer	Requires complicated control functions to capture heat transfer from outside of standpipe	Accurately models both sides (inside and outside) heat transfer
Radiation heat transfer	Thermal radiation transfer between standpipes does not account for the steam external of the standpipes	Thermal radiation transfer between standpipes does account for the steam external of the standpipes
Oxidation	Does not model the oxidation of the outside of the standpipe	Accurately models oxidation on both inside and outside surfaces
Flow area	Debris is limited to the area within the standpipe	Debris can fill areas both inside and outside standpipe

A major drawback of modeling the standpipes as canister components is that the channel boxes within the core and the standpipes would be made of the same material. Zircaloy plays a key role in severe accidents with respect to oxidation (heat and hydrogen generation), and it contributes to the overall degradation behavior of the core and ex-vessel molten core-concrete interaction (MCCI). Substituting the channel box material with stainless steel or swapping the standpipe material with Zircaloy were measures that were deemed to be inappropriate approximations. Thus, the standpipes were modeled as SS.

The bottom support of the steam dryers was also modeled as a PLATE type SS. The steam dryers were modeled as COLUMN type SS.

Control functions were established to account for the heat transfer from the standpipe SS and the shroud head to the volume outside the standpipes. If the water were 50 mm deep or greater in the control volume next to the structure, heat transfer from the SS to the water was specified based on the SS surface area, the temperature difference between the SS and the control volume, and an assumed heat transfer coefficient of 3,000 W/m^2 K. Otherwise, if water were less than 50 mm deep in the control volume next to the structure, heat transfer from the SS to the control volume was specified based on the SS surface area, the temperature difference between the SS and the control volume, and an assumed heat transfer coefficient of 100 W/m^2 K. The heat flows in either direction, depending on the temperature difference. Once an SS fails, the heat transfer to the external control volume is stopped, and it is allowed to relocate via particulate debris with the heat transfer as determined internally by MELCOR. Implementation of this semi-empirical heat transfer model accounted for approximately 1,200 new lines of input in the plant model.

An additional 45 core cells (COR) were added to the existing non-UI model. As shown in Figure 1, five cells were used in modeling the shroud dome, 25 included the steam separator SS, and 15 were used to model the steam dryers. In general, the UIs were distributed between the five radial rings of core cells (COR package) based on the cross sectional areas of the rings.

In this effort, 45 control volume hydrodynamic (CVH) cells were created. As shown in Figure 2, 5 cells were used in modeling the space near the shroud dome, 15 were used for the space occupied by the steam separators, 15 were used to model the volume outside the steam separators, 5 were used to model the space above the steam separators and the bottom support of the steam dryers, and 5 were used to model the steam dryer space.
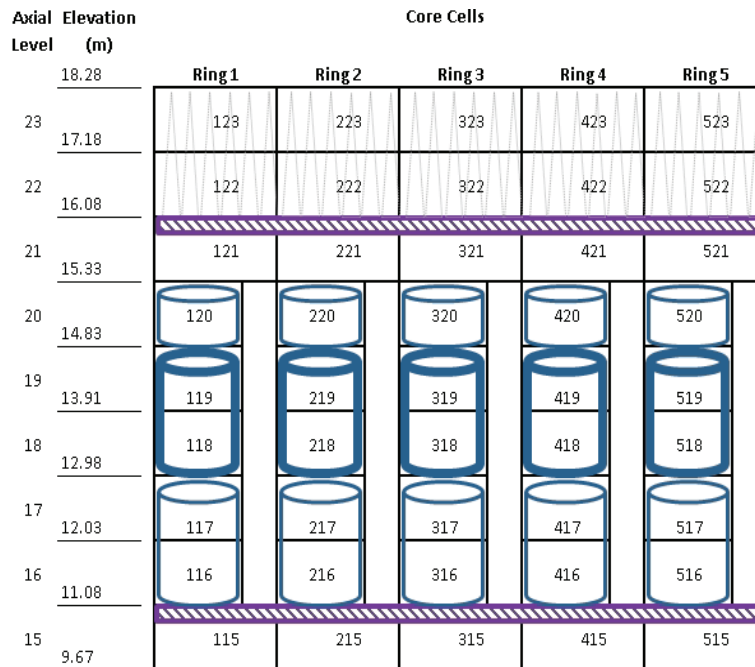

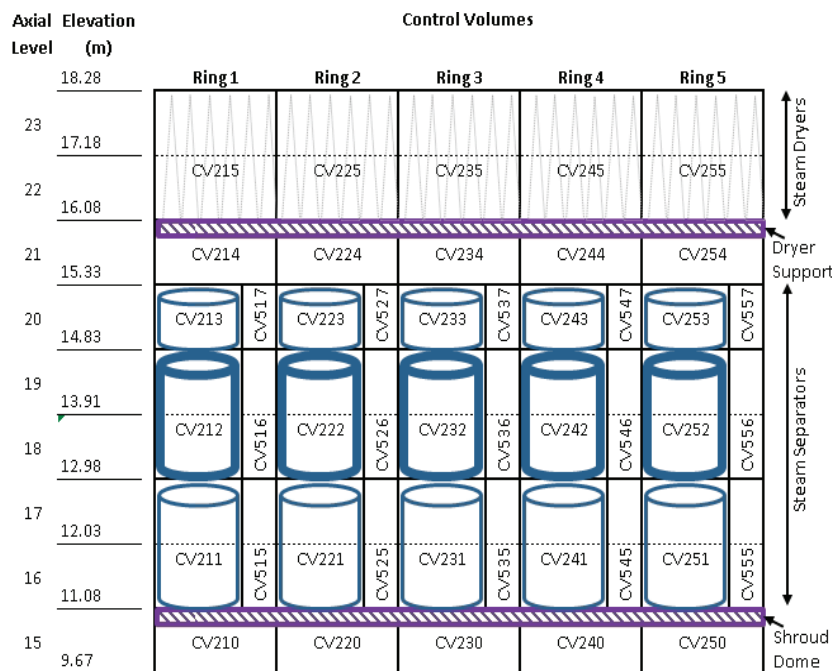**Figure 1. COR Cell Discretization for UIs.**

Figure 2. Control Volume Discretization for UIs.

Table IV. Summary of additional flow paths to model the UIs

Num.	Type	Connection Description	Example
5	Axial	Shroud dome free space to the steam separator standpipes	CV210-CV211
5	Axial	Shroud dome free space to the regions external to the steam separator standpipes. These only open if the shroud dome fails.	CV210-CV515
10	Axial	Control volumes within the stand pipes	CV211-CV212
10	Axial	Regions external to the steam separator standpipes to each other	
5	Axial	Outlet of the steam separator stand pipes to the free space above the standpipes	CV213-CV214
5	Axial	Outlet of the regions external to the steam separator standpipes to the free space above the standpipes	CV517-CV214
5	Axial	Outlet of the free space above the standpipes to the steam dryers	CV214-CV215
5	Axial	Outlet of the steam dryer exits to the steam dome	CV215-CV360
4	Radial	Shroud dome free space to each other	CV210-CV220
4	Radial	Free space above the steam separators to each other	CV214-CV224
4	Radial	Steam dryers to each other	CV215-CV225
12	Radial	Regions external to the steam separator standpipes to each other	CV515-CV525
15	Radial	From the region inside to the region outside the steam separator standpipes. These only open if sections of standpipes fail. The separator region (CV212) is assumed to be open 5% to the external space during normal operation.	CV211-CV555
5	Radial	Steam dryers to the outer annulus, water return	CV215-CV310
4	Radial	Steam separators to the outer annulus, water return	CV557-CV310

For the periphery shroud heat structures (RPV, shroud, or other structure), 10 heat structures either needed to be added or modified. These heat structures needed to conform to the COR discretization used.

An additional 98 flow paths (FL) were added to the model and are briefly summarized in Table IV. Control function logic was added to open select flow paths if a component failed. Flow paths were opened if (1) the component temperature exceed 1,700 K (the SS melting temperature), or (2) the remaining life of the structural component calculated by MELCOR was equal to 0.0 (see manual for description [3]).

2.4.3. Component stress and failure modeling

Supporting structures can fail in MELCOR through yielding, creep, and in the case of columns, buckling. The yield strength and elastic modulus are based on temperature-dependent equations. The default values, based on 304 stainless steel, are provided in Figure 3.

The stress of the PLATE type SS is conservatively assumed to be a simply supported, uniformly loaded, flat circular plate, as shown in Eqns. (1, 2), where i refers to the core ring number, r is the core ring radius, W is the weight the plate is supporting, h is the plate thickness, and K_0 and K_1 are coefficients with default values of 0.206 and 0.576, respectively. Once the calculated stress for a core ring exceeds the yield strength, the plate is assumed to fail. The plate material in that ring, as well as all the SS the ring supported, is converted into particulate debris. For PLATE type SS, when a ring fails, all inner rings also fail; however, rings external to the failed ring can remain standing.

$$\sigma_i = 6 \cdot K_0 \cdot \frac{1}{\pi \cdot h^2} \cdot W \qquad\qquad \text{for i=1} \qquad (1)$$

$$\sigma_i = 6 \cdot K_0 \cdot \frac{1}{\pi \cdot h^2} \cdot \left[1 - K_1 \left(\frac{r_{i-1}}{a} \right)^2 \right] \left[1 + \left(\frac{r_0}{r_{i-1}} \right)^2 \right] \cdot W \qquad \text{for i>1} \qquad (2)$$
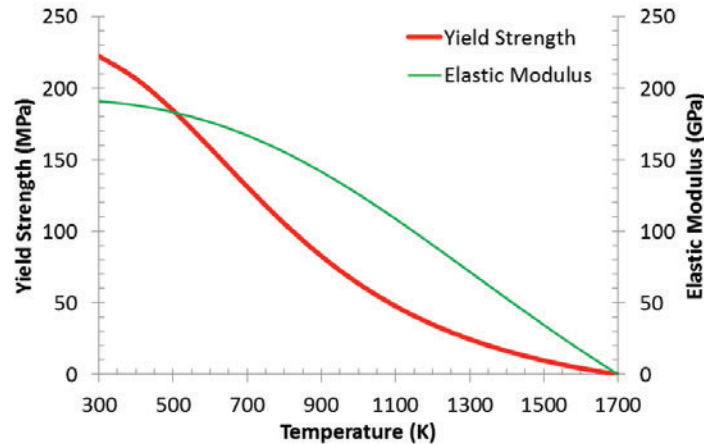
Figure 3. Default Yield Strength and Elastic Modulus.

Assuming that the shroud dome is a flat circular plate with simply supported edges is likely an overly conservative assumption for the actual geometry. For comparison, for a spherical head with a uniform loading (force per unit of tangential area, q) with tangentially supported edges, the stress is given by Eqn. (3) [8]. A spherical head represents an ideal geometry with respect to structural loading. For a hemispherical head that has been truncated at 45° from the central axis, the maximum stress for a uniform loading (force per unit of tangential area, q) with tangentially supported edges, is given by Eqn. (4) [8]. Using the dimensions of the shroud head given in Table I, Eqn. (1, 3, 4) are compared in Table V.

$$\sigma_{max} = \frac{1}{2} \cdot \frac{r}{h} \cdot q \tag{3}$$

$$\sigma_{max} = \frac{\pi \cdot \sqrt{2}}{2} \cdot \frac{r^3}{h} \cdot q \tag{4}$$

Table V. Comparison of maximum stress for various geometries under uniform tangential loading

Geometry	Maximum stress per loading q	Ratio of stress compared to flat plate
Flat plate, simply supported	3,739	-
Hemispherical, 45°, tangential support	954	0.255
Hemispherical, 90°, tangential support	27.5	0.007

As with the shroud dome, the base of the steam dryers were also modeled as a flat circular plate with simply supported edges. However, the corrugated construction of the steam dryers would act to increase the area moment of inertia giving the structure increased capacity to resist bending moments compared to a flat plate.

As modeled, the stress calculations for the shroud dome and steam dryers are conservatively high. Detailed geometry information and finite element methods are necessary to perform realistic stress analysis of the UIs. To accommodate the approximate stress modeling available in MELCOR compared to the actual stresses in the UIs, a range of simulations were performed in which the calculated stress for the PLATE type SS was scaled to be 1×, 0.1× and 0.02× that calculated for a simply supported circular flat plate.

MELCOR contains a simple stress model for predicting buckling of multiple parallel columns. This model was used in the modeling of the separator standpipes and steam dryers. MELCOR also contains a creep model that is based on the Larson-Miller creep-rupture model. For further descriptions of these models, see the MELCOR manuals [3].

The default melting temperature for stainless steel in MELCOR is 1,700 K, and the melting point of the oxide is 1,870 K. These default values were used for the melting failure mode.

3. ANALYSIS RESULTS

Four cases were simulated. The first case, "original model," is the unedited model without the addition of the new UI modeling. The second case, "UI model," is with the UI modeled as described in Section 2.4. The third case, "UI model – 0.1× stress," and the fourth case, "UI model – 0.02× stress," include the UI modeling; however, the calculated stress in the shroud dome and the support for the steam dryers were reduced by factors of 10× and 50×, respectively. See Section 2.4.3 for a discussion of the modeling used to determine stresses.

3.1. Heat up of the upper internals

Steam and hydrogen are generated during a station blackout as the coolant boils away and the core materials oxidize. The hydrogen is heated and the steam is superheated as they pass up through the core. Figure 4 illustrates the gas temperature in the top-central control volume within the core region for the "original model" case. These hot gases then pass through the UIs on their way out through an SRV (or a break). It is these hot gases, in addition to thermal radiation from the core region, that have the potential to heat the UIs to high temperatures.
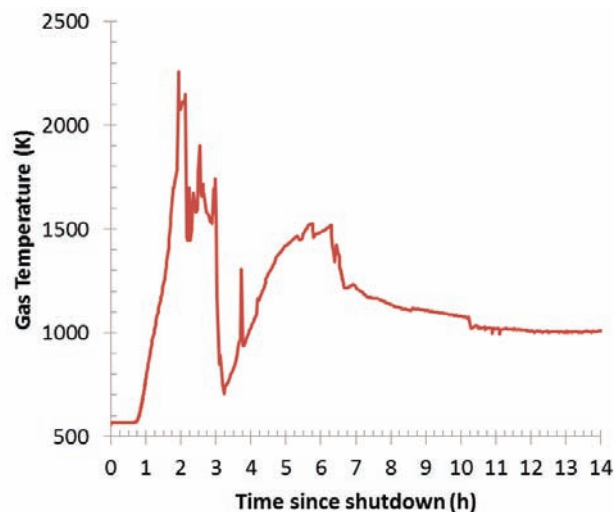

Figure 4. Gas Temperature in the Top-central Core Region, Original Model Case.

The temperature of the intact UI structures for each COR cell (see Figure 1) are plotted in Figure 5 for the four cases. When the structure fails in a COR cell, the temperature is illustrated as falling to zero. The initial heat up rates of the UI are similar between all cases. This is expected, as the structures have similar mass and surface areas, as well as similar superheated steam and hydrogen heat sources from below. In the "original model" case, shown in Figure 5A, the UIs reach a maximum temperature of approximately 1,425 K in around 2.5 h. As the water level drops below the active fuel height (Figure 6),

the production of steam decreases, as well as the heat generated through oxidation of the core structures. The ability to superheat the steam decreases as the core slumps. Note the decrease in gas temperature in the 2–3 h timeframe in Figure 4. The decreased flow and temperature of gases up through the UIs results in the UI temperatures stabilizing around the 2–3 h timeframe (Figure 5A). As the core material relocates into the lower plenum, a large amount of steam is generated. This steam passes through the voided core region without much additional heat added to the gasses, and then it passes through the UIs. These relatively colder gases cool the UIs, as seen in Figure 5A, during the 3–4 h timeframe. However, as the water drops in the lower plenum, the ability to heat the hydrogen and superheat the steam increases, and the temperature of the gases passing through the UIs increases, as seen in the 3.5–6.5 h timeframe in Figure 4 and Figure 5A. After the lower head dries out and fails, most of the heat source is removed from the vessel. However, some radionuclides are volatilized during the core degradation process, and some deposit onto the UIs. These radionuclides can continue to heat the UIs over time.
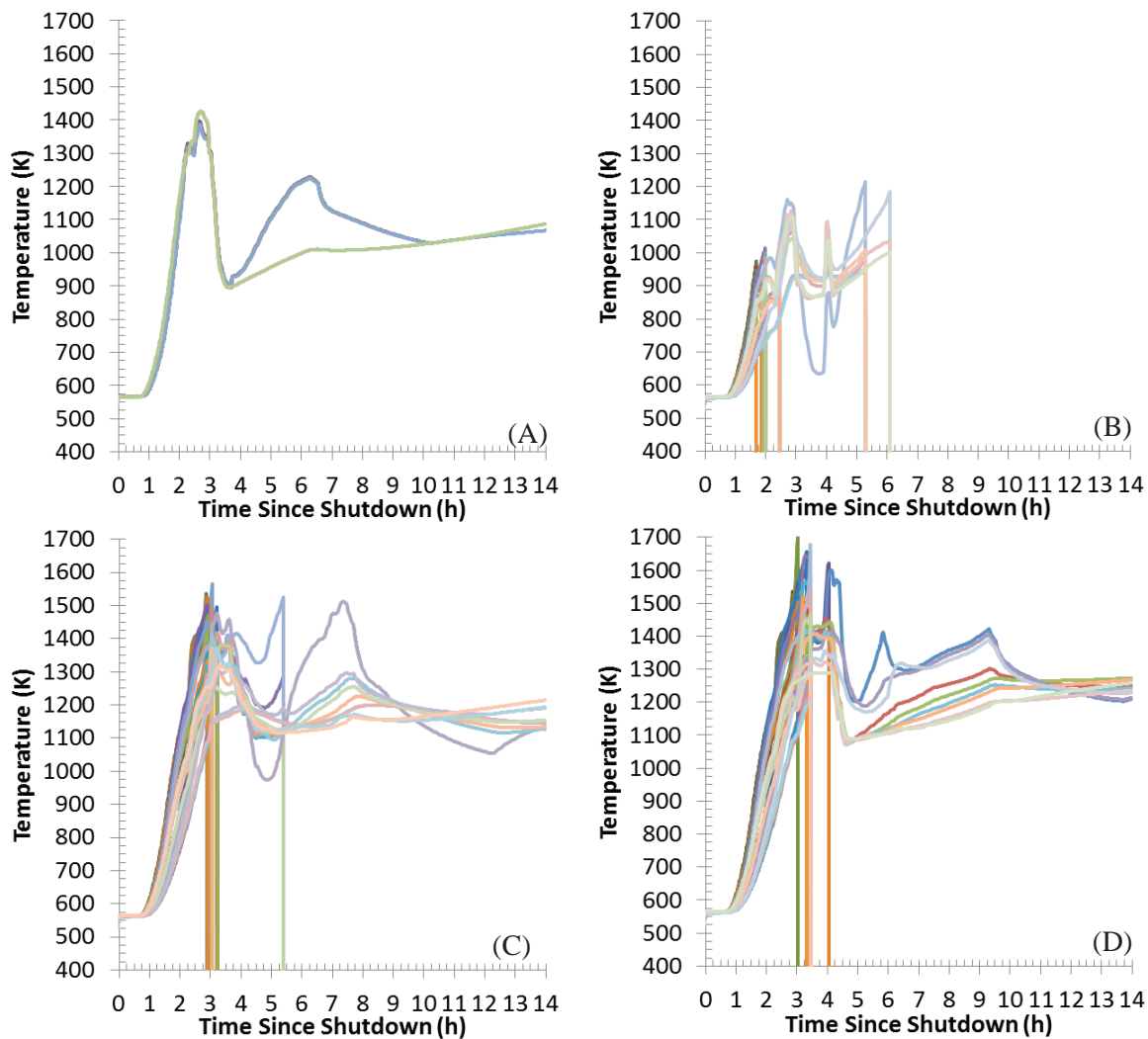
Figure 5. Intact SS Temperatures for Original Model (A); UI model (B);
UI model - 0.1× Stress in Plates (C); UI Model - 0.02× Stress in Plates (D).

The cases including the new UI model follow a similar progression as the "original model" case. However, the UIs can relocate, affecting the core degradation process below. Also, the structures are

discretized finer, with their geometry more accurately modeled, providing for higher fidelity prediction of the structures' heat up.

For the "UI model" case, Figure 5B, the PLATE type SS (the shroud dome and base of dryers) for the shroud dome are predicted to begin failing quite early. The central ring fails after reaching approximately 830 K, with subsequent rings failing soon after at slightly higher temperatures. The bases of the dryers fail soon after at temperatures of approximately 780 K. After the PLATE type SS fails, the structures above (i.e., the separators or dryers) are modeled as no longer being supported, and they subsequently fail.

As noted is Section 2.4.3, the predicted stresses in the PLATE type SS are likely overestimated in the model compared to the actual geometry. For the "UI model – 0.1× stress" case, the PLATE type SS remains intact longer but begins to fail at temperatures of 1,400–1,525 K. For the "UI model – 0.02× stress" case, the PLATE type SS remains intact much longer; however, it is predicted to reach very high temperatures approaching the melting point.
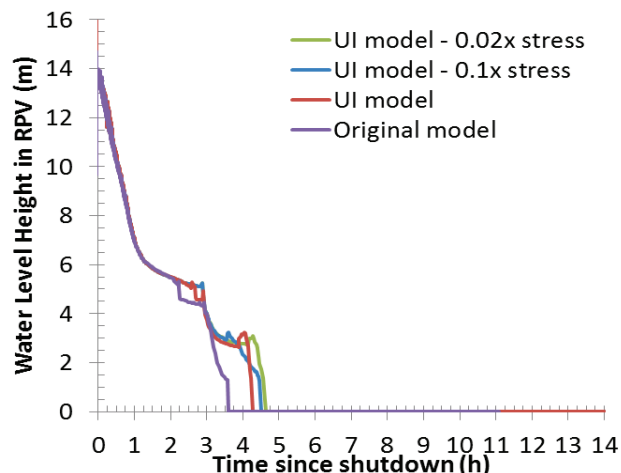

Figure 6. Water Level in RPV.

3.2. Failure Timing

Figure 8 illustrates the temperatures and failure progression of the core and UI regions for the original model, UI model, and UI model–0.05× stress cases at specific times during the accident. The temperatures listed are for the intact cladding in the core region and the intact SS in the UI region. When the UI SS or the cladding fails, the cell is illustrated as empty.

In the cases using the new UI modeling, the top level of the core stays cooler than in case of the original model (see Figure 8, 1.5 h and 2.0 h). This is attributed to differences in the axial heat transfer from the top level of the core to the shroud dome. This results in the cladding at the top level of the core failing later with the new UI modeling than in the original model.

Table VI summarizes the timing of the first failure of various structures. The initial failure mode is indicated for the SRVs and containment. As expected, the timing of the first cladding rupture is similar between simulations. For the UI model, the shroud dome and dryers fail before the first failure of the channel box and cladding relocation. For the UI model – 0.1× stress case, the shroud dome fails at a similar time as the channel box and cladding. Finally, for the UI model – 0.05× stress case, the shroud

dome fails after channel box and cladding. The differences of relocation timing impact the downstream core degradation and oxidation process.

Table VI. Timing of First Failure of Structures

Structure	Case timing (min)			
	Original Model	UI Model	UI Model 0.1× stress	UI Model 0.02× stress
Cladding rupture	77	79	79	79
Channel box	115	140	175	173
Cladding relocate	117	155	177	175
Shroud dome	NA	102	174	181
Steam dryers	NA	111	192	181
SRV	175[a]	173[b]	171[b]	171[b]
Lower head	377	460	447	558
Containment	392[c]	474[c]	461[c]	569[d]

[a] Cycles at high temperature; [b] large number of cycles; [c] liner melt through; [d] drywell head flange leak.

3.3. In-vessel hydrogen generation

The approximately 100 tons of stainless steel in the UIs represent a potentially large source of hydrogen if oxidized. In the "original model" case, the heat structures used to model the UIs cannot oxidize. Conversely, the UIs can oxidize in the cases with the new UI modeling. Figure 7 provides the cumulative hydrogen generated inside the RPV. The timing of relocation of the UIs impacts both the generation rate and the total amount of hydrogen generated in-vessel. When the UIs relocate into the core region, the stainless steel material competes with the Zircaloy for steam with respect to oxidation. The oxidation of stainless steel is less exothermic than the oxidation of Zircaloy. These effects impact the total amount of hydrogen generated in-vessel and the amount of energy released due to oxidation. Ultimately, the oxidation of the stainless steel in the new UI model contributes approximately 500 kg of additional hydrogen, or approximately +25%.
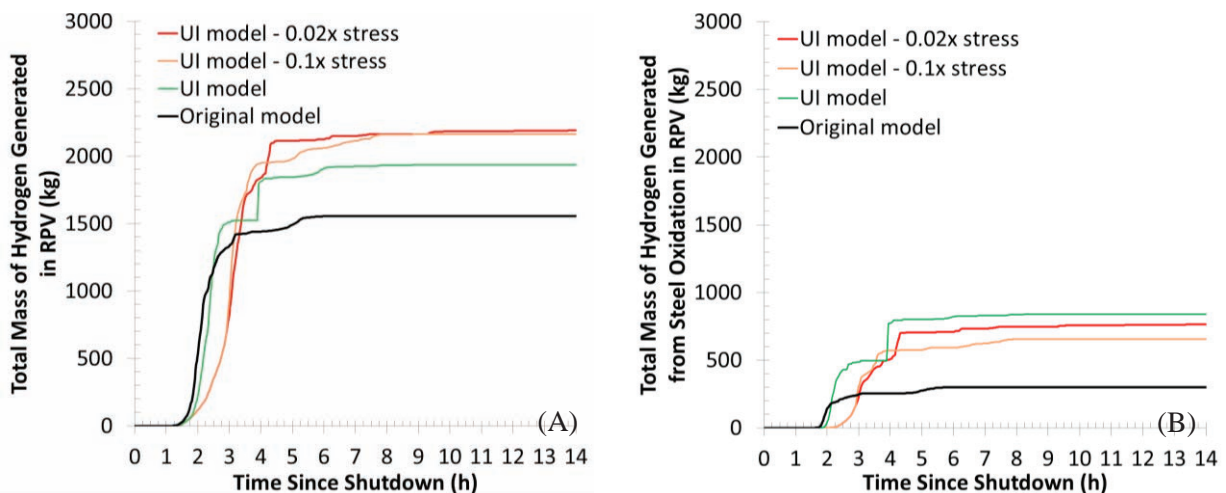

Figure 7. Cumulative Hydrogen Generated In-vessel; (A) total, (B) by stainless steel.

Time: 1.5 h   2.0 h   3.0 h   4.0 h   6.0 h

Original model

Dryers
Separators
Dome

Core Region

UI model

Dryers

Separators

Dome

Core Region

UI model – 0.05× stress
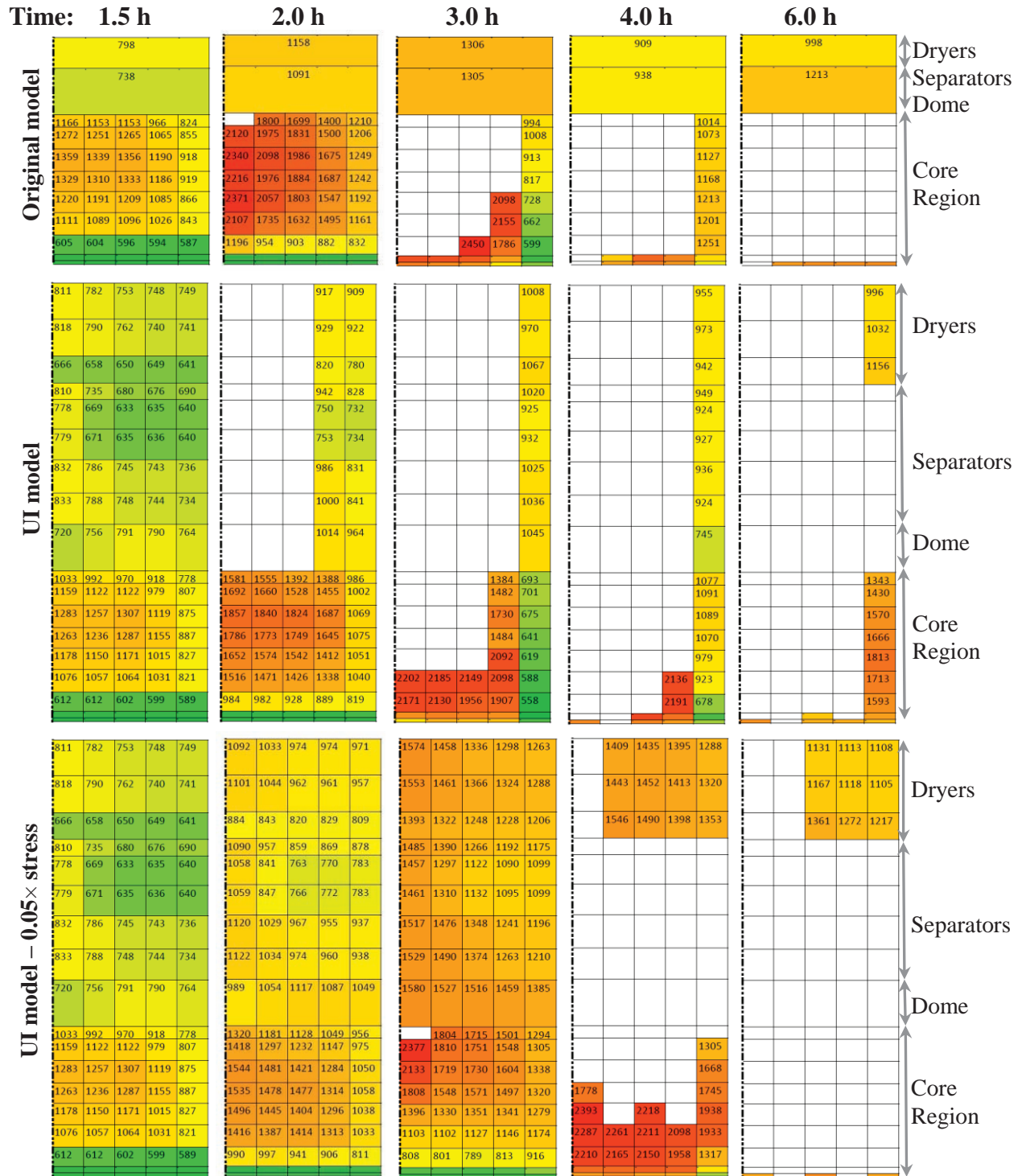
Dryers

Separators

Dome

Core Region

Figure 8. Core and UI Temperature (K) and Failure Progression for the Original Model Case, UI Model Case, and the UI Model - 0.05× Stress Case.

3.4. Ex-vessel Effects

The cumulative mass of material ejected from the bottom head is provided in Figure 9. Allowing for the UIs to relocate contributes a large amount of addition material ex-vessel.
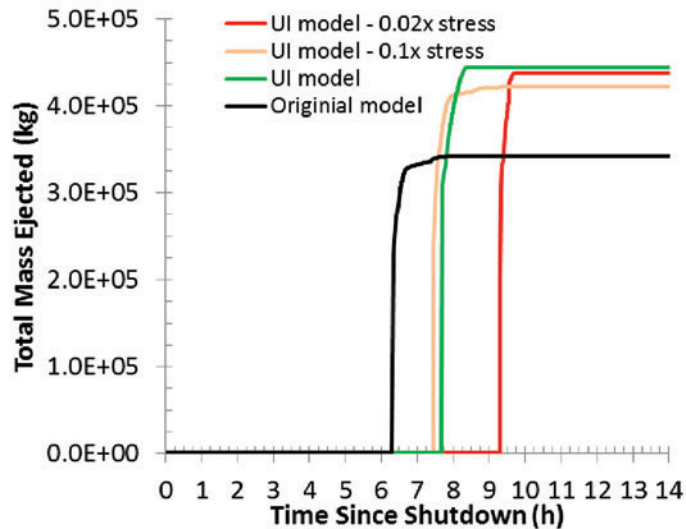
Figure 9. Cumulative mass of melt release from the RPV

The ex-vessel modeling, with respect to melt spreading and the stabilization of MCCI, is limited in MELCOR 1.8.6 and in available versions of MELCOR 2.1 as of this writing [9]. The additional steel and steel oxides would alter the thermophysical properties of the melt. The oxidation of the additional steel that is ex-vessel represents a large potential source of additional hydrogen and carbon monoxide. Intuitively, the amount of melt that relocates could impact the distance the melt spreads and its depth. Previous sensitivity studies have noted the high importance of the melt depth with respect to melt coolability [10]. More detailed analysis is required to understand the impact of the additional UI material on the ex-vessel accident progression.

4. DISCUSSION AND CONCLUSIONS

The major findings of the study are summarized as follows. A model for the UI was developed for use in MELCOR. A number of issues were identified while developing this model. The shroud dome, separators, and dryers are predicted to reach high temperatures during the modeled STSBO. The UIs reached temperatures high enough that the structures have very limited structural loading capacity. Based on the conservative structural mechanics modeling available in MELCOR, the UIs are predicted to fail and relocate downwards. The timing of relocation ranged from prior to major core degradation to just after the start of core degradation. The relocation of the UIs impacted the amount of hydrogen generated (generating approximately 500 kg more, or about +25%), the timing of the core and vessel degradation process, and the amount of melt ejected from the vessel. The additional ex-vessel melt, approximately 100 tons, has the potential to impact the melting spreading, cause more aggressive MCCI and generating additional non-condensable and flammable gases.

Similar to the results of this study, 29 years ago, a study using the MARCON code with a purpose-built finite element model predicted that the shroud dome could heat up to high temperatures [1]. The previous study notes the importance of various heat transfer modes. In particular, the entrance region of the steam separator standpipes may have 3× higher convective heat transfer than in the fully developed region, an effect not taken into account in the MELCOR modeling.

The heat up of the UIs is directly related to the heat transport from the core to the upward flowing gases. A recent crosswalk exercise explored the differences between the MELCOR v2.1 and MAAP5.02 severe accident codes with respect to core degradation [11]. Due to differences in modeling, MELCOR predicts

higher transfer of heat to the gases and much higher temperatures in the steam dome. Thus, a similar study of the upper internal response during severe accidents using the MAAP5.02 code may result in lower predicted upper internal temperatures.

Additional analysis using more rigorous modeling (i.e., finite elements) of UI structural integrity at elevated temperatures is recommended. The manner in which the UIs may slump and the subsequent impact on flow paths should be further investigated. These higher fidelity studies could provide guidance and form the basis for simpler modeling representations used in systems level codes such as MELCOR.

As noted, the relocation of 100 tons of additional material ex-vessel has the potential to impact the loads on containment. Future modeling using tools specifically designed to model melt spreading, and the long-term coolability of the core debris would provide insight into the potential impact.

Inspection and decommissioning of Units 1–3 at Fukushima Daiichi provide for a unique opportunity to understand the response of the UIs during severe accidents. Lower fidelity integral modeling (i.e., MELCOR), higher fidelity separate effects modeling (i.e., finite element for the structural response of the UIs and specialized codes for ex-vessel phenomena), and observations from inspections at Fukushima Daiichi could provide the technical basis for understanding the response and role of the UIs during severe accidents.

ACKNOWLEDGEMENTS

REFERENCES

1. US Nuclear Regulatory Commission, "State-of-the-Art Reactor Consequence Analyses Project; Volume 1: Peach Bottom Integrated Analysis," NUREG/CR-7110, **1** (2012).
2. E. W. Barnes, M. Keyhani, and L. J. Ott, "Response of the BWR Shroud Head Under Severe Accident Conditions," Letter Report to NRC T. J. Walker (1986), publication pending.
3. MELCOR Computer Code Manuals, Version 1.8.6, NUREG/CR-6119, Rev. 3, Sandia National Laboratories, Albuquerque, NM (2005).
4. K. R. Robb, "Updated Peach Bottom Model for MELCOR 1.8.6: Description and Comparisons," ORNL/TM-2014/207, September 2014.
5. US Nuclear Regulatory Commission, "Severe accident risks: an assessment for five US nuclear power plants," NUREG-1150, US Nuclear Regulatory Commission, Washington, DC (1990).
6. Tennessee Valley Authority, "Browns Ferry Nuclear Plant Updated Final Safety Analysis Report," amendment 18, November 16, 1999.
7. T. Tamakoshi, N. Watanabe, and M. Hirano, "Development of input data for thermal-hydraulic computer code TRAC-BF1 for analyses of 1,100MW BWRs," JAERI-DATA/CODE–98-037, pp. 201 (1998).
8. T R. J. Roark and W. C. Young, *Formulas for Stress and Strain*, 7th Ed., McGraw Hill, New York (2002).
9. K. R. Robb, M. T. Farmer, and M. W. Francis, "Ex-Vessel Core Melt Modeling Comparison between MELTSPREAD-CORQUENCH and MELCOR 2.1," ORNL/TM-2014/1 (2014).
10. K. R. Robb and M. L. Corradini, "Ex-Vessel Corium Coolability Sensitivity Study with CORQUENCH Code," Proc. of NURETH-13, ANS, Sept. 27–Oct. 2, Kanazawa, Japan, paper N13P1290 (2009).
11. D. Luxat, J. Hanophy, D. Kalanich, and R. Wachowiak, "Modular Accident Analysis Program (MAAP) – MELCOR Crosswalk, Phase 1 Study," Electric Power Research Institute, 3002004449 (2014).